CHAPTER 11

LIVING MARINE RESOURCES APPLICATIONS

R. MICHAEL LAURS
National Marine Fisheries Service
Southwest Fisheries Center
La Jolla, California

JOHN T. BRUCKS
National Marine Fisheries Service
Fishery Engineering and Development Division
National Space Technology Laboratories
NSTL Station, Mississippi

1. INTRODUCTION

Satellite oceanic remote sensing is beginning to play an important role in fishery research and fishery management by providing synoptic oceanic measurements for use in evaluating environmental effects on the abundance and availability of fish populations. Variations in ocean conditions play key roles in natural fluctuations of fish stocks and in their vulnerability to harvesting (Hela and Laevastu, 1961, 1970). Information on the changing ocean, rather than on average ocean conditions, is necessary to understand and eventually model the effects of the ocean environment on fish stocks (Sette, 1961). This knowledge is required to provide the best possible advice in making fishery management decisions and to develop efficient harvesting strategies for fishery resources.

The use of satellite remote sensing in oceanography expanded considerably in the 1970s and satellites with dedicated oceanographic sensors were first launched in 1978. Coincident with the developments in satellite oceanography, there have been substantial increases in demand on the marine waters of the United States for activities such as fisheries development and utilization, recreation, and offshore oil exploration. With these increased activities have

ADVANCES IN GEOPHYSICS, VOLUME 27

ISBN 0-12-018827-9

come expanded requirements for living marine resource-management programs through legislative mandates such as the Marine Mammal Protection Act of 1972, the Fisheries Conservation and Management Act of 1976, and the Ocean Pollution Research Development and Monitoring Act of 1978. With these responsibilities, there has been an increasing need to design and initiate improved ocean-monitoring programs for resource management. The capabilities of evolving satellite remote-sensing technology, combined with conventional data collection techniques, provide a powerful tool for the efficient, cost-effective management of living marine resources.

Remote sensing is not entirely new to fishery scientists nor to fishermen harvesting living marine resources. Mariners learned long ago they could increase their perspective by elevating themselves above the water's surface. Fishermen have done this by use of crow's nests on ships, hot-air balloons, and aircraft. The sensor often used has been the naked eye, usually aided by a telescope or binoculars. Visual forms of remote sensing are common today in many fisheries, e.g., the use of helicopters operating from modern tuna purse seiners fishing on the high seas. In addition, aircraft carrying instruments for making oceanographic measurements have been used for supporting fisheries research studies (Pearcy, 1973; Thomas, 1981; and others), for locating areas favorable for fishing (Squire, 1961, 1972; and others), and for locating schools of fishes (Squire, 1982; and others).

The era of space technology brought new perspectives in remote sensing for fisheries. Man acquired the ability to view entire oceans and seas in a matter of minutes. Early satellite remote-sensing investigations for fisheries used information gathered over the ocean by systems designed for making terrestrial and meteorological observations. The objectives of these studies were to determine if certain satellite sensors could measure or identify selected oceanographic features believed to influence the distribution of fish. For example, early feasibility investigations were conducted to evaluate if fish distribution patterns may be related to temperature and color measurements made by satellites, e.g., the ERTS-1 menhaden investigation (Kemmerer *et al.*, 1974), the Skylab-3 game fish investigation (Savastano *et al.*, 1974), and the Landsat menhaden and thread herring investigation (Brucks *et al.*, 1977).

The recent development of satellite remote-sensing techniques for fisheries applications employs data from active and passive instrumentation which has been or is presently aboard a number of satellites. A wealth of satellite remote-sensing systems exists today. For the most part, however, satellite remote-sensing applications in fisheries have concentrated on the measurements of ocean temperature and color, and computation of ocean transport based on satellite-measured wind stress. Synoptic coverage of ocean temperature, color, and wind stress by no means represents the entire spectrum of environmental information necessary or required for fisheries applications.

However, knowledge of key oceanographic conditions and processes affecting the recruitment, distribution, abundance, and harvests of fishery resources may often be deduced using these data.

The purpose of this chapter is to review published living marine resource applications of ocean measurements made by Seasat and the Nimbus-7 Coastal Zone Color Scanner (CZCS). In addition, recent U.S. research involving the use of satellite infrared thermal data in fisheries is described. Satellite ocean remote-sensing applications in fisheries research is treated first and then the utilization of satellite data in fisheries-aid products that are distributed to fishermen.

2. Satellite Ocean Remote-Sensing Applications in Fisheries Research

The resolution capabilities of remote-sensing systems carried by spacecraft are not adequate for direct detection of fish schools. This has necessitated fishery scientists to examine ocean features that can be measured with spaceborne sensors and in turn can be used in fishery resource investigations. The use of satellite infrared thermal data, scatterometer wind-stress measurements, and Coastal Zone Color Scanner measurements in fisheries research investigations is yielding results which demonstrate that satellite oceanic remote sensing can be an important tool in fisheries research.

2.1. Use of Satellite Infrared Thermal Data in Fisheries Research

Satellite infrared thermal data are playing an increasingly important role in fisheries research. It is being used by U.S. fishery scientists to (1) define marine habitats of fishery resources using satellite data, which are collected contemporaneously with fishery/biological data and ground truth measurements gathered by research and fishing vessels; and (2) describe and explain variability in circulation and water mass distributions using satellite data alone or in conjunction with physical oceanographic measurements, with a view toward understanding the influence of ocean variability on fishery resources and fishing grounds.

2.1.1. Use of Satellite Infrared Imagery for Describing Ocean Processes in Relation to Spawning of the Northern Anchovy. Satellite infrared imagery was used by Lasker *et al.* (1981) for describing ocean processes in relation to spawning of the northern anchovy (*Engraulis mordax*). In this study NOAA-6 satellite thermal imagery of the Pacific Ocean adjacent to the United

States–Mexico west coast was collected on a daily basis coincident with fine-grid oceanographic ship observations. Shipboard observations included sampling of anchovy eggs, larvae, and adults as well as physical oceanographic measurements, e.g., continuous monitoring of temperature and salinity, discrete surface temperature measurements, and measurement of subsurface temperature profiles. The objectives of the investigation were to relate variations in mesoscale sea surface-temperature distributions with anchovy spawning and to identify and delineate ocean processes that might be important to the survival of fish eggs and larvae, e.g., upwelling (Lasker, 1978) and offshore transport (Parrish and MacCall, 1978).

Based on satellite imagery and confirmed by shipboard observations during the study, which was conducted during a peak period in anchovy spawning, there were distinct temperature regimes in the general geographic region where anchovy spawning normally takes place. There were (1) a cold area resulting from upwelling off Point Conception and north, (2) a large warm area which extended from Baja California into the Southern California Bight and approximately 185 km offshore, and (3) a large area of the bight with intermediate surface temperatures. The mesoscale features of surface temperature changed slowly so that for a given day the temperature distribution apparent in a satellite image did not appear to be markedly different from the preceding or following few days.

Figure 1 (from Lasker *et al.*, 1981) is an infrared thermal image which has superimposed on it the geographic distribution of anchovy egg catch. The distribution of just-spawned anchovy eggs clearly showed that nearly all spawning was confined to the Southern California Bight and to a band 40 km wide, parallel to the Baja California coast. The seaward extent of spawning in the bight was apparently abridged by the southward intrusion of recently upwelled water indicated by the 14°C isotherm. Also, anchovies were excluded from the water warmer than 17°C beyond 40 km of the Baja California coast. The satellite temperature/anchovy egg relationships were corroborated by mapping the distribution of first-day eggs on sea surface temperature observations made concurrently aboard ship.

Relatively high numbers of anchovy larvae were found in plankton hauls taken by another research vessel in the coastal area north of Point Conception in February 1980. Temperatures were very warm for this entire zone in February, with progressively warmer conditions to the south. Winds were light and from the south prior to March 11 and upwelling was minimal. Winds from the north increased on March 12 and persisted. When the area north of Point Conception, where anchovy larvae had been collected in February, was sampled in March, no larvae of any age were found. This suggested to the authors that the extensive upwelling, as indicated by wind data and observed by satellite, carried anchovy larvae out of the coastal zone

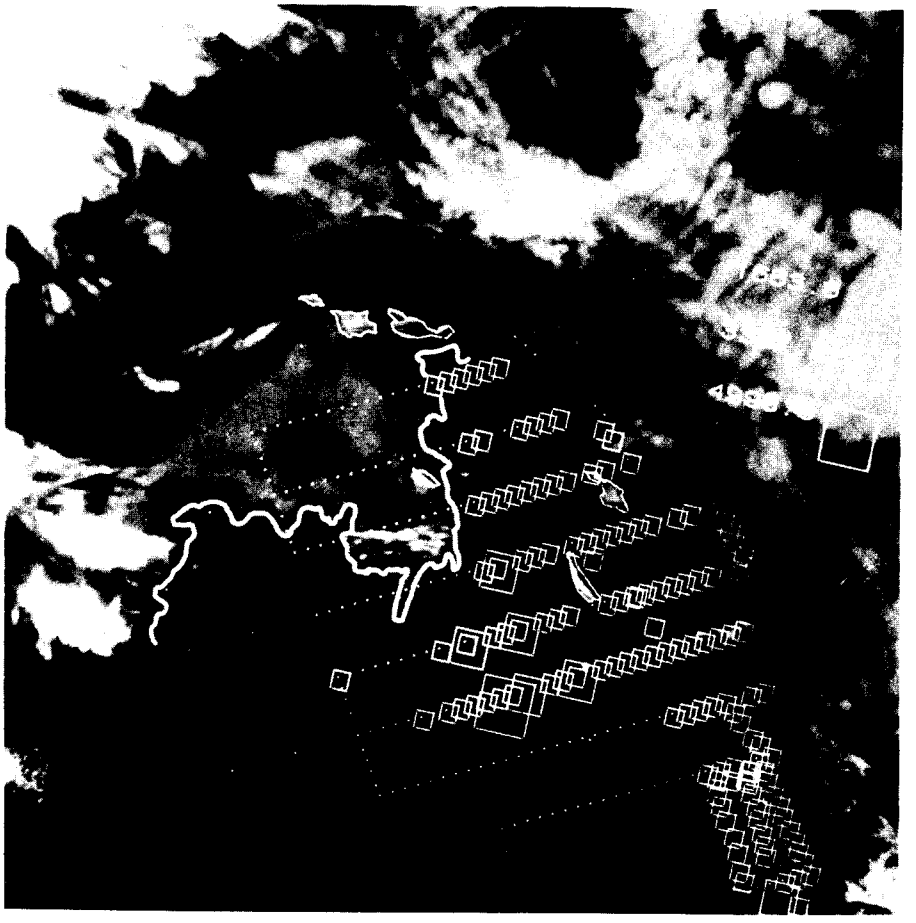

FIG. 1. Distribution of anchovy eggs superimposed on NOAA-6 infrared thermal image of the Southern California Bight. The 14°C isotherm plotted from satellite gray-scale calibration has been drawn in. Feathery objects are clouds. Square indicates number of anchovy eggs under 1 m^2 of sea surface. (From Lasker *et al.*, 1981.)

and into the California Current. At the same time adult anchovies were excluded, as was evidenced by lack of fish in trawl samples. The start of upwelling on March 14 and the progressively colder temperatures appeared to have excluded anchovies from that time on. Lasker *et al.* concluded that anchovy avoid recently upwelled water and that the areal extent of upwelled water may be mapped using infrared satellite imagery. They stated:

> Because satellites can see vast areas of the ocean day in and day out, they provide the scientist with a synoptic look at processes only seen heretofore on smaller scales and restricted to the time when a ship or ships can cover the area of interest. In this study only a

satellite could have provided us with a synoptic picture of the large scale oceanographic events which were happening over the entire spawning area of the anchovy during the peak of the spawning season. The extensive ground truth provided by the R/V *David Starr Jordan* confirmed that the 0.5°C accuracy of the infrared radiometer aboard most of the NOAA satellites detects accurately the movement of surface layers and shows the sequential development of upwelling along the California coast over large areas of ocean [Lasker *et al.*, 1981].

Satellite remote sensing has also been utilized by Fiedler (1983) to investigate variations in spawning habitat of the northern anchovy in the Southern California Bight. He found that spawning in the northwestern region of the bight is excluded from a cold-water mass apparent in infrared satellite imagery south of Point Conception, corroborating the earlier findings of Lasker *et al.* (1981), and that spawning to the south is confined to coastal waters with moderately high phytoplankton pigment levels as measured by the CZCS. (The latter will be discussed further in Section 2.3.) Fiedler (1983) also concluded that satellite images can be used to improve the sampling efficiency of ichthyoplankton surveys. The effectiveness of using satellite infrared and CZCS imagery (see Section 2.3) to monitor shifts in anchovy spawning habitat off California associated with the 1982–1983 El Niño warm-water conditions have been demonstrated by Fiedler (1984a,b).

2.1.2. Use of Satellite Infrared Thermal Imagery in Tuna and Billfish Studies. Satellite infrared thermal imagery has proved to be a valuable tool in tuna research. This has been especially true in studies designed to investigate relationships between tuna distribution and availability and ocean temperature fronts and sea surface temperature.

2.1.2.1. North Pacific albacore tuna distribution in relation to ocean temperature fronts. Albacore tuna (*Thunnus alalunga*), which are highly mobile and widely distributed in the North Pacific, migrate seasonally into waters off the coast of North America during July through October where they support important commercial and recreational fisheries. Laurs *et al.* (1984) used Advanced Very High Resolution Radiometer (AVHRR) infrared thermal data from the NOAA-7 satellite and fishery data from logbooks kept by commercial albacore tuna fishermen to investigate relationships between albacore fishing success and oceanic temperature fronts in waters off California. Relationships to ocean-color boundaries were also examined using CZCS imagery (Section 2.3). Laurs *et al.* found that fishing effort and highest catch rates for albacore tended to be concentrated in the vicinity of temperature fronts, which are believed to result from coastal upwelling (Fig. 2). High catch rates were observed on the warm side of the temperature boundaries, usually very near the boundary but sometimes extending up to 100 km offshore from the boundary or front. Fishing activity was markedly less and catch rates were

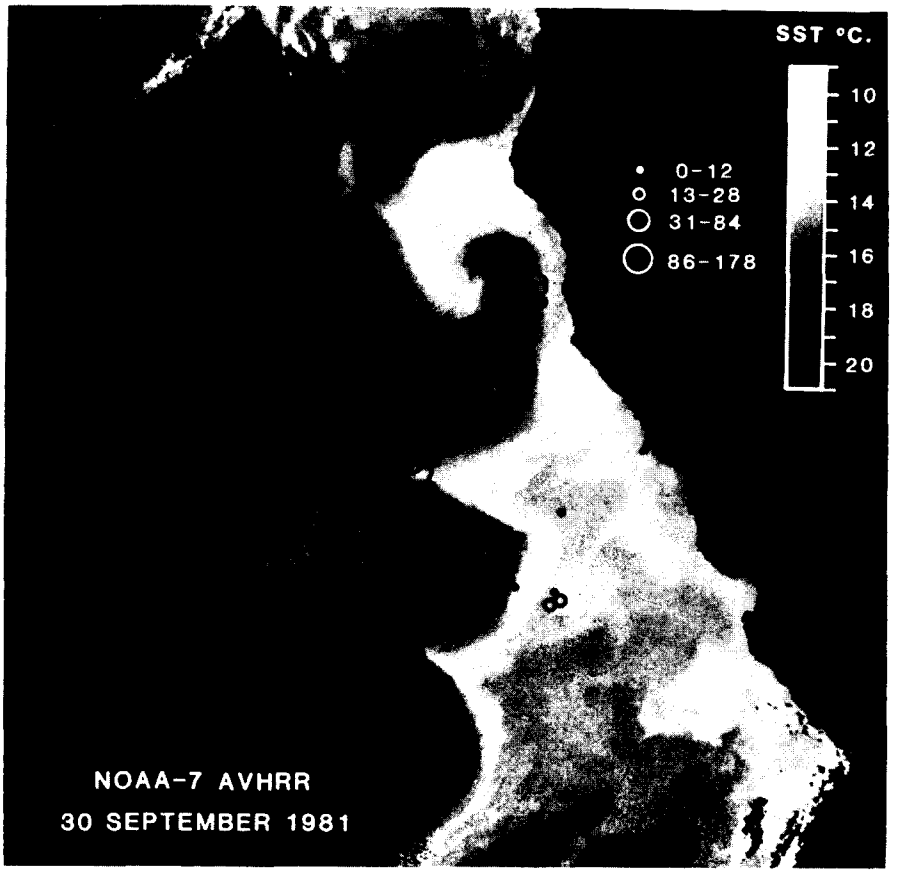

FIG. 2. Distribution of mean daily albacore tuna catches made by commercial fishing vessels superimposed on NOAA-7 AVHRR image of water off central California. Albacore catch rates are expressed as number of albacore caught per 150-line hours of fishing and are shown as varying sizes of circles. (From Laurs *et al.*, 1984.)

usually nil on the cold side of the temperature fronts (Fig. 2). While it is generally believed by fishermen and fishery scientists that tuna may aggregate in the vicinity of upwelling temperature fronts to feed (Laurs *et al.*, 1977), the use of satellite imagery is allowing fishery scientists to investigate this relationship on space and time scales hitherto not possible.

Laurs and Austin (1985) investigated the small-scale migration patterns of albacore in relation to oceanic frontal boundaries using ocean color and infrared satellite data collected contemporaneously with observations made from ships at sea. Nimbus-7 CZCS and NOAA-6 satellite AVHRR infrared data were collected in conjunction with field experiments where acoustic telemetering methods were used to track the horizontal and vertical move-

ments of free-swimming albacore, and expendable bathythermograph (XBT) observations were made to determine subsurface ocean thermal structure. Three albacore were tracked for approximately 24 hr and one for about 15 hr. The results showed that (1) total distances tracked ranged from about 40 to 60 km, with all fish remaining in the same parcel of warm water that was separated from waters to the north, south, and inshore by about a 2°C temperature gradient as shown by infrared thermal imagery; (2) tracked fish spent most of the time in waters within and below the thermocline, and only small amounts of time in the upper mixed layer; (3) the fish exhibited marked vertical excursions in depth, with the range being larger during the day than at night; (4) the fish spent most time in waters with temperatures considerably lower than what has been generally believed to be the preferred temperature range for albacore; and (5) when changing depth, the fish, frequently within a 20-min period, passed through a vertical gradient of temperature amounting to 6–7°C or about 3+ times greater than the horizontal temperature gradient at the surface indicated by ship measurements and the infrared thermal imagery.

These findings indicate that the reasons tuna aggregate on the warm side of surface temperature fronts—an economically significant phenomenon that has been observed on scientific cruises and is well known by fishermen—may not be related to thermal–physiological mechanisms (Neill, 1976). Instead, Laurs and Austin speculate that one or more behavioral mechanisms related to feeding may be responsible. Ocean-color measurements made by the CZCS in conjunction with the tracking study and with catches made by commercial fishing vessels (Laurs *et al.*, 1984) provide data that support this hypothesis (see Section 2.3).

Laurs *et al.* (1981) report on another study involving albacore tuna which was conducted in winter several months after albacore emigrate from waters near the North American coast. In this study NOAA-6 infrared thermal imagery was used in conjunction with fish catch information and ground truth measurements made by chartered commercial albacore fishing vessels. The investigators found that a marked temperature front observed in the satellite imagery appeared to be a boundary to albacore distribution. There was up to a 20-fold decrease in catch rate on the cool side of a temperature front believed to mark the outer edge of the California Current approximately 700 miles off southern California.

2.1.2.2. Gulf of Mexico tuna longline fishery and the Loop Current. Leming (1981) evaluated the feasibility of using satellite imagery to locate the position of the Loop Current in the eastern Gulf of Mexico in an investigation of relationships between the Loop Current and tuna caught by the Japanese longline fishery. The locations of longline sets and species composition of

the catches were recorded by National Marine Fisheries Service (NMFS) observers on board selected vessels of the Japanese longline fleet operating in the Gulf of Mexico. GOES-East satellite infrared images composited weekly and analyzed for major thermal boundaries by the NESS Satellite Field Service Station in Miami, Florida, were used to estimate the position of the Loop Current. An apparent strong correlation was found in early May 1978 between sets targeted on bluefin tuna and the location of surface thermal boundaries of the Loop Current (Fig. 3; Leming, 1981). However, after late May or early June, surface temperature gradients in the Gulf of Mexico were of insufficient magnitude to be detected in the GOES imagery. Curiously, during this period, all fishing for bluefin tuna ceased, and fishing was targeted for yellowfin tuna in the western Gulf of Mexico. For the most part Leming had only limited success finding a relationship between the Loop Current and tuna longline fishing in 1979.

According to Leming (1981) the thermal boundary charts he used based on GOES infrared imagery did not contain sufficient resolution in time and space for use in an analysis of catch-rate differences for major pelagic groups of fish in relation to satellite data. He concluded that to correlate catch rates with satellite data the thermal boundary analyses must be expanded to include secondary thermal gradients, ground resolution less than 8 km must be used, and composite time scales less than 1 week are necessary. The GOES provides overall the best data source, however, because the frequency of data allows compositing for cloud-cover removal, a more serious problem than spatial resolution (Maul *et al.*, 1984).

2.1.2.3. Atlantic bluefin tuna distribution in relation to seasonal ocean warming. Roffer *et al.* (1982) used satellite remote sensing in conjunction with shipboard observations and fishing logbook records in an investigation of Atlantic bluefin tuna (*Thunnus thynnus thynnus*) off the coasts of the mid-Atlantic states. Using satellite infrared imagery to follow the seasonal northerly progression of the 19–20°C surface isotherms, Roeffer *et al.* found that the development and duration of the various bluefin tuna fisheries along the East Coast follow the movement of seasonal warming of near-surface waters.

2.1.2.4. Movements of Atlantic swordfish in relation to ocean features. Carey and Robinson (1981) conducted tracking experiments of a swordfish with acoustic telemetry instruments to investigate the daily patterns in activity. Satellite infrared imagery was collected in conjunction with the tracking to study the movements of swordfish in relation to ocean features. Among the oceanic features apparent in satellite imagery were cold shelf water, warm Gulf Stream waters, and a streamer of cold shelf water pulled off by the Gulf Stream moving past Cape Hatteras. The swimming direction of

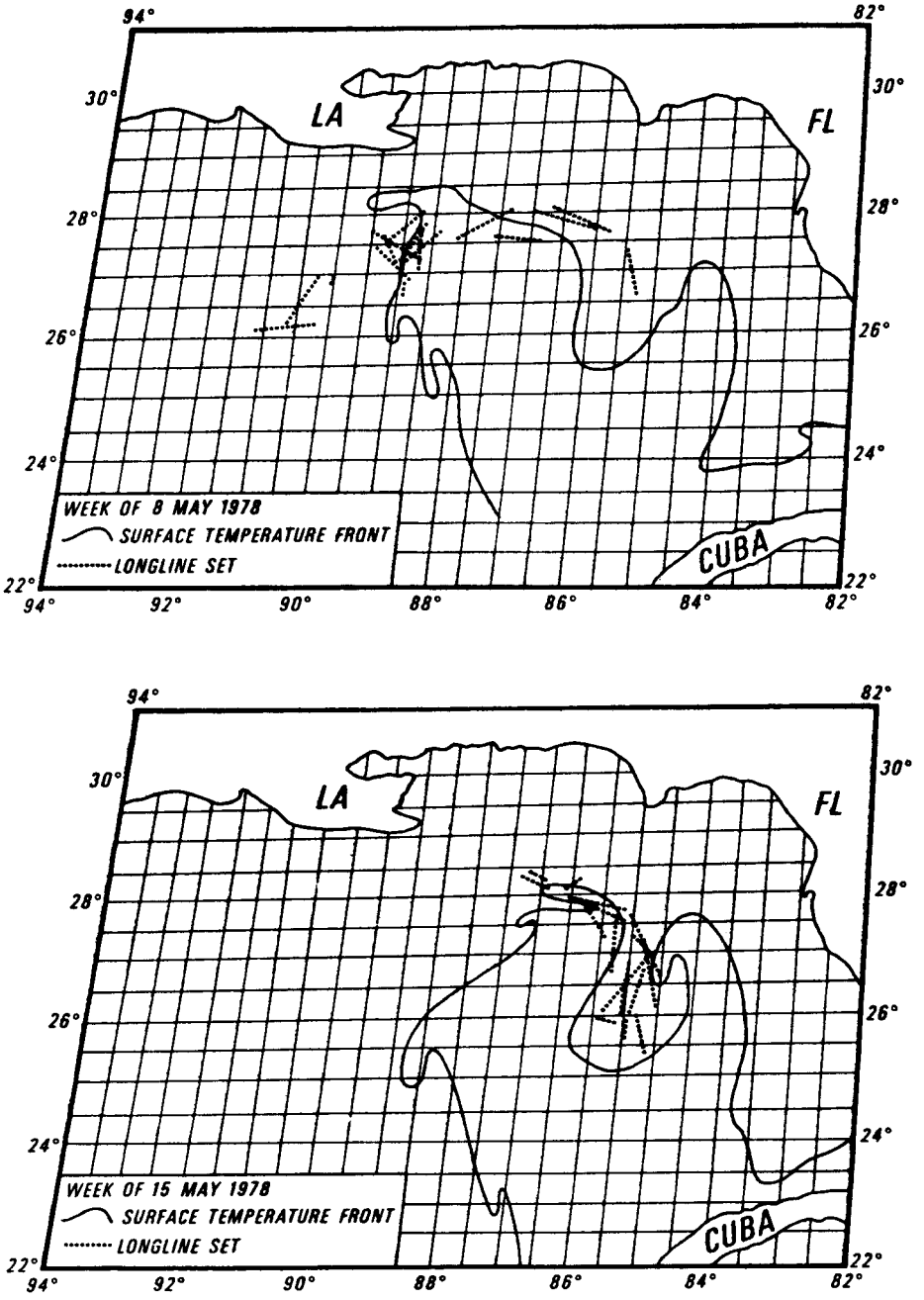

FIG. 3. Distribution of longline sets relative to the May 1978 position of the Loop Current boundary in the Gulf of Mexico deduced from GOES infrared satellite imagery. (From Leming, 1981.)

the swordfish for the 3-day period it was tracked was not correlated with oceanic surface thermal boundaries obvious in the infrared image. The tracked fish was tagged on the north side of entrained cold shelf water and after tagging it swam across the cold shelf water and the Gulf Stream, and then into the Sargasso Sea.

The horizontal swimming pattern of the swordfish did not appear to be influenced by oceanic boundaries between different types of waters as has been observed in albacore tuna (Laurs and Austin, 1985). This difference in the relationships between oceanographic environmental conditions and the movements of swordfish and albacore tuna became apparent largely because satellite imagery was collected contemporaneously with the tracking experiments.

2.2. Modeling Larval Transport Mechanisms Using High-Resolution SASS Wind-Stress Measurements

Brucks *et al.* (1984) conducted a case study using Seasat-A Satellite Scatterometer (SASS) wind data to establish, quantify, and document the extent and variability of wind-induced ocean-flow indices on surface-layer transport. Knowledge of surface-layer transport processes is important in fisheries research because dispersal mechanisms control the distribution of early life stages and thereby influence the recruitment and future harvest of marine organisms with planktonic life stages. The purpose of the case study was to determine whether high-resolution SASS measurements of wind stress could improve estimates of surface layer and larval transport based on geophysical models.

The study was conducted in the Gulf of Mexico where surface layer transport plays a key role in the early survival of shrimp and menhaden. Fisheries on these species in the Gulf produce the major portions of the highest U.S. dollar and largest U.S. volume fishery. In addition, several other economically important commercial fisheries in the Gulf have planktonic life stages which are influenced by prevailing dispersal mechanisms common to all. A schematic representation of the penaeid shrimp life cycle is given in Fig. 4 showing transport of developmental stages from offshore regimes to coastal estuarine zones and the adults returning offshore to spawn.

2.2.1. Description of Model and Preparation of SASS Input Data. Brucks *et al.* (1984) developed a model to use sea surface wind stress measured by the SASS to calculate surface-layer transport. The Seasat approach developed by Brucks *et al.* compared to the standard technique for deriving surface transport is shown in Fig. 5. The Seasat approach reduces the number

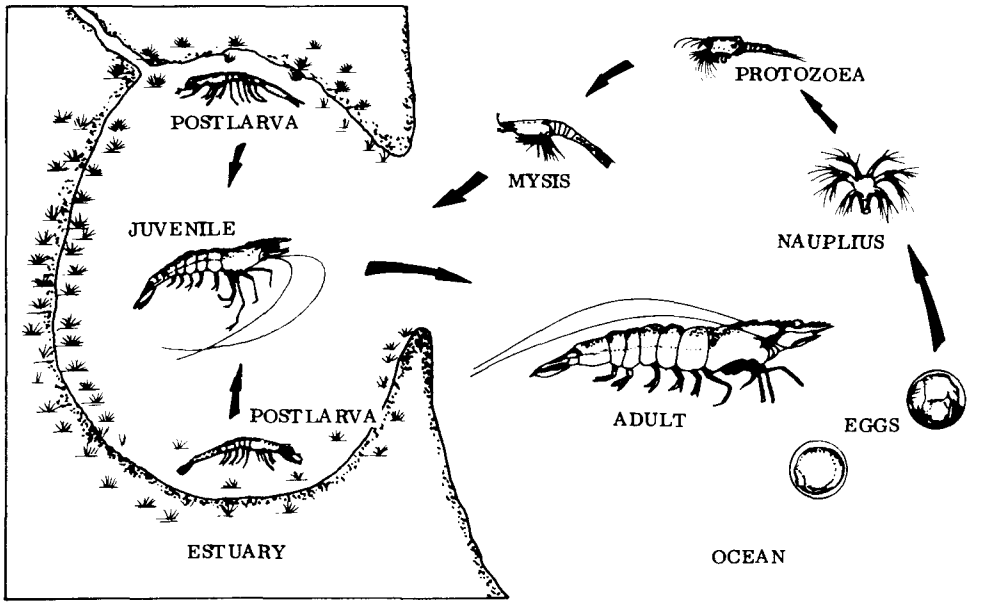

FIG. 4. Life cycle of penaeid shrimp showing transport of developmental stages from offshore to coastal estuarine zones and adults returning offshore to spawn. (From Brucks *et al.*, 1984.)

of assumptions involved in the calculation of the wind-stress vector and presumably provides more accurate estimates of surface circulation. The model is composed of offshore and coastal modules to satisfy deep and shallow water responses to meteorologic driving forces. Hydrographic boundary conditions are essentially fixed by monthly and/or seasonal averages of historical temperature and salinity data. Surface transport is thus a function of the varying wind field.

The SASS data set for input to the model of surface-layer transport was compiled by extracting scatterometer wind measurements from 70 revolutions over the Gulf of Mexico during September 1978. The spatial distribution of these 11,248 SASS measurements in the study area available for analyses is shown in Fig. 6.

The geophysical data records for scatterometer wind measurements with the direction alias removed were stratified into 26 5-day running averages grided by $\frac{1}{2}^\circ$ square. Analyses showed that sufficient coverage of the Gulf is attained within 5 days. Longer periods added to the data density, but did not improve the distribution of data.

The SASS-measured wind-stress field was used to calculate surface currents by the standard homogeneous, steady-state Ekman (1905) solution.

Model outputs consist of 5-day mean current vectors on a $\frac{1}{2} \times \frac{1}{2}^\circ$ grid. A trajectory analysis package is also available to portray current pathways of

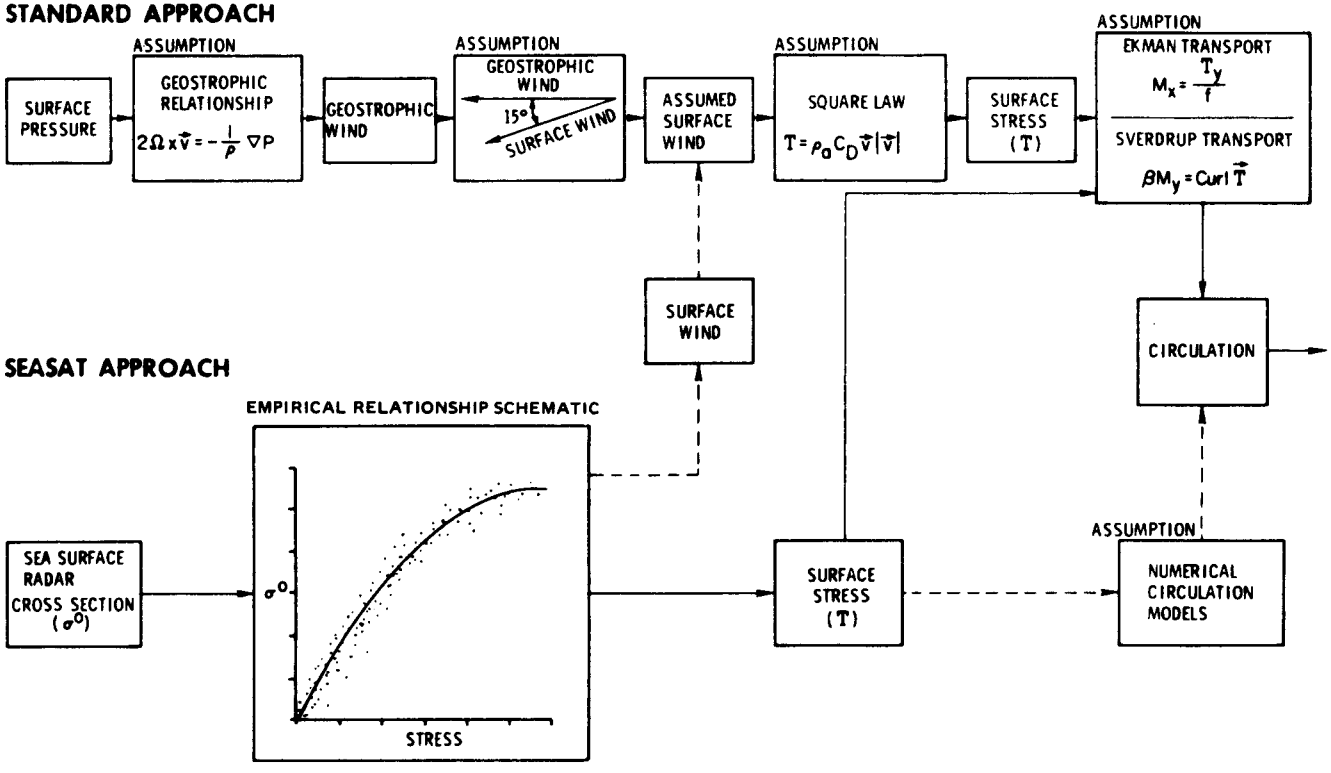

FIG. 5. Comparison of Seasat and standard technique for deriving surface-layer transport. (From Brucks *et al.*, 1984.)

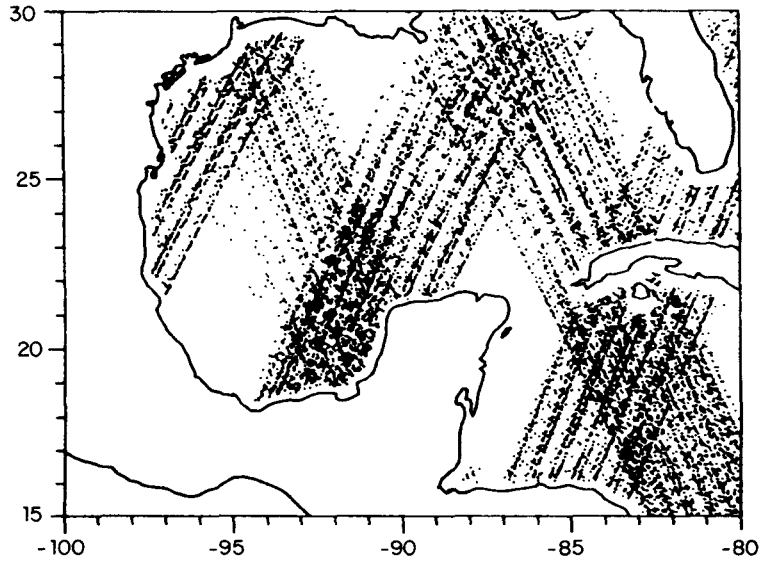

FIG. 6. Spatial distribution of 11,248 SASS measurements of the Gulf of Mexico for September 1978. (From Brucks *et al.*, 1984.)

eggs and larvae and to define impact areas. The trajectory analysis allows random selection of any number of starting points, tracking of the dispersal routes, and demonstration of the impact area of particle location between 1 and 30 days of drift. The wind-driven surface currents derived from SASS observations can be used independently for studies of wind-driven circulation or can be combined with surface flow estimates from thermohaline models to produce total current transport at the ocean surface.

Fields of vertical velocity representing upward velocity into the Ekman layer required to balance the computed Ekman divergence induced by the wind-stress curl may also be output from the model. The vertical movement of water due to wind-stress curl provides insight for the enumeration of environmental factors relevant to dispersal mechanisms for fisheries. Divergence in Ekman transport will cause upwelling of waters possibly rich in nutrients, thereby creating areas of high productivity. Conversely, convergence in the Ekman layer will produce downwelling, forming areas of accumulation of planktonic organisms. The relationship between the curl of wind stress and the vertical movement of water is important also in the delineation of spawning areas. Historically, geographic boundaries of spawning areas are identified generally by those zones high in egg and larvae concentrations and/or high in adult specimens laden with mature eggs or possessing mature, "ripe" ovaries (i.e., ready to spawn). Correlation between

wind-stress curl and concentrations of planktonic eggs and larvae could assist in the definition of spawning areas. In this fashion, source ambiguities could be resolved to show that the observed concentration is due to local spawn or is due to a consequence of environmental redistribution and accumulation of distant spawn.

2.2.2. Estimates of Surface-Layer Transport and Vertical Movement of Water Using SASS Wind Data. Using SASS wind stress to calculate surface-layer transport processes showed striking spatial and temporal variability in wind-drift patterns and regions of convergence/divergence in the Gulf of Mexico. During the first half of September, surface wind drift was most pronounced in the northwestern Gulf. Initially, surface flow was oriented toward the northwest (Fig. 7a). By midmonth the wind-drift regime increased in aerial coverage and changed direction such that anticyclonic flow prevailed in the western Gulf (Fig. 7b). An obvious change occurred again in the third week as evidenced by the regional shift of predominant wind drift to the southwest quadrant of the Gulf, including the Yucatan Straits, and a change in wind-drift direction to the northwest and north (Fig. 7c). Additionally, the magnitude of the wind-driven circulation throughout the Gulf increased approximately twofold with a mean and maximum velocity of 10.50 and 45.71 cm sec^{-1}, respectively. At the close of the month (Fig. 7d), the wind-driven circulation regime was sluggish. A southwest drift current, indicating a current reversal, was present in the northwest Gulf, replacing a northerly current identified previously, and an area of prominent wind-driven activity was apparent for the first time in the northeast Gulf.

Estimates of the curl of the wind stress based on the SASS measurements showed the Gulf to have a highly dynamic oceanic system of regional convergence and divergence. Using the Seasat data base the Gulf was convergent and divergent about equal amounts of time (approximately 1.5:1), with mean and maximum vertical velocities (cm sec^{-1}) of 5.2×10^{-4} and 31.4×10^{-4}, respectively. Using the standard method and data base the Gulf was almost always convergent (approximately 4:1), with lower mean and maximum vertical velocities (cm sec^{-1}) of 3.0×10^{-4} and 14.2×10^{-4}, respectively.

Brucks *et al.* used the SASS model derivations of wind-driven surface-layer transport processes to define potential enrichment zones of spawn material and predict the areas of coastal impact of eggs and larvae as controlled by environmental forces. Processes conducive for the offshore accumulation of planktonic organisms were found mainly in the western and eastern Gulf (Fig. 8). The western distribution was concentrated generally in the west central Gulf with projections to the south, west, and north. Distributions in

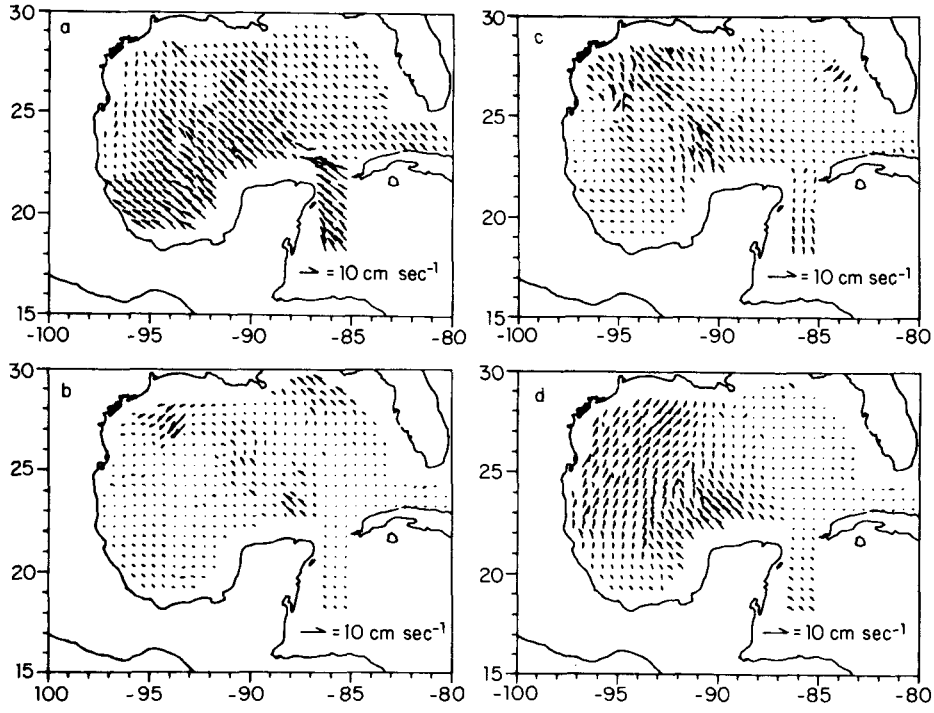

FIG. 7. Wind-driven circulation patterns show variability resulting from SASS data for four 5-day periods during September 1978. (a) Day 263 = days 261–265 (or September 20 = September 18–22); wind-stress average (dynes cm^{-2}) = mean 0.93, max 4.00; current-speed average (cm sec^{-1}) = mean 10.50, max 45.71. (b) Day 270 = days 268–272 (or September 27 = September 25–29); wind-stress average (dynes cm^{-2}) = mean 0.29, max 2.75; current-speed average (cm sec^{-1}) = mean 3.14, max 31.44. (c) Day 250 = days 248–252 (or September 7 = September 5–9); wind-stress average (dynes cm^{-2}) = mean 0.48, max 1.83; current-speed average (cm sec^{-1}) = mean 5.42, max 20.87. (d) Day 256 = days 254–258 (or September 13 = September 11–15); wind-stress average (dynes cm^{-2}) = mean 0.60, max 2.04; current-speed average (cm sec^{-1}) = mean 6.87, max 23.28. (From Brucks *et al.*, 1984.)

the east were separated although large, discrete areas prevailed in the eastern Gulf and Yucatan Straits. Coastal accumulations, summarized in Fig. 9, occurred in the northwest Gulf off Texas, Louisiana, and Mississippi; the southwest Gulf off Mexico; and in the east Gulf off Florida. Trajectories due to oceanic and wind effects shown in Fig. 8 were merged to compare final impact areas to areas of known nursery grounds (Fig. 10). It was shown that predicted impact areas were in close proximity to nursery grounds in Louisiana, Texas, and Florida.

2.2.3. Usefulness of Seasat SASS Wind-Stress Measurements in Modeling Larval Transport Mechanisms. Brucks *et. al.* concluded that Seasat afforded

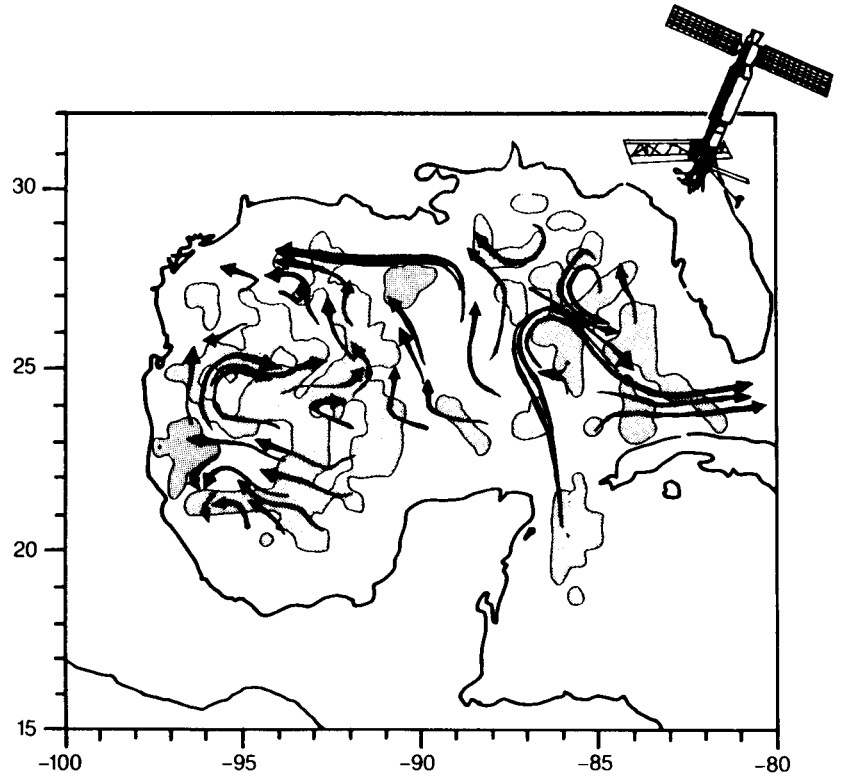

FIG. 8. High-probability area for offshore waters rich in planktonic eggs and larvae due to accumulations by wind-driven convergence of surface waters (shaded regions). Surface current trajectories are superimposed to show 30-day dispersal pathways for September 1978. (From Brucks *et al.*, 1984.)

new technology for fisheries application to monitor, model, and predict environmental pathways by which offshore spawn of estuarine-dependent shellfish and finfish find their way into coastal nursery grounds. Synoptic and repetitive direct measurements of wind stress provided enhanced capability to determine wind-driven environmental events, including a pertinent measure of inherent variability, that influence recruitment processes of marine organisms and provide a means to correlate significant interactions between subregions in the Gulf of Mexico. The effect of dispersal mechanisms is common to all major fisheries that have planktonic life stages and knowledge of transport processes can, therefore, help satisfy basic mission requirements of the NMFS for management of national fisheries and for the negotiation and establishment of international agreements concerning fisheries that span national boundaries.

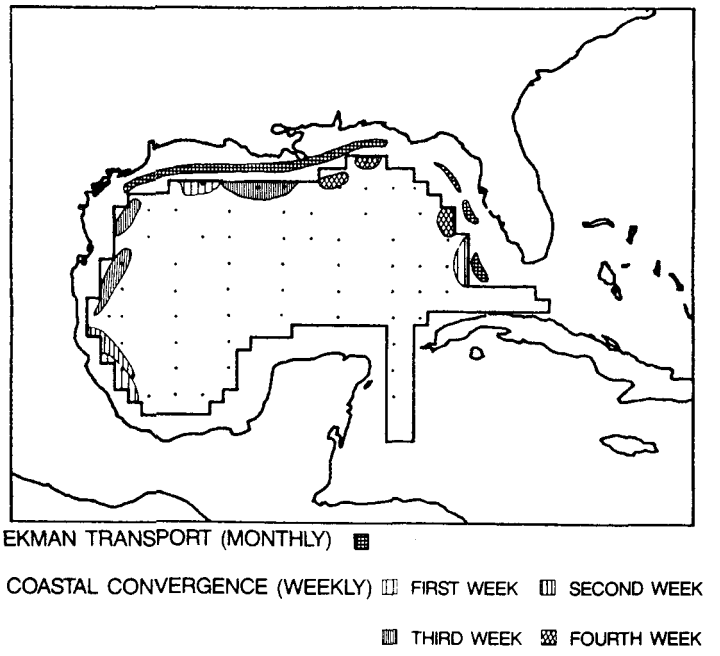

FIG. 9. High-probability area for coastal waters rich in eggs and larvae for September 1978. (From Brucks *et al.*, 1984.)

2.3. Use of Coastal Zone Color Scanner Data in Fisheries Research

The concept of using ocean color for finding fishing grounds is not new. Fishermen have used variations in ocean color for centuries to locate oceanic areas believed to be favorable for catching fish. The potential value to fishermen of synoptically acquired ocean-color data from space was first demonstrated by Kemmerer *et al.* (1974). In this study ocean-color measurements from Landsat were used to predict areas of high probability of occurrence of menhaden in the Gulf of Mexico.

When the Nimbus-7 satellite with the CZCS was launched in 1978 there was increased enthusiasm and interest by fishery scientists to utilize satellite ocean-color measurements in fisheries research. Cram (1979) speculated on the use of CZCS measurements in the management of a pelagic fishery. However, applications of CZCS imagery to fisheries research has only recently been realized with the increased availability of CZCS data and improved access to hardware and software to process the color imagery.

Ocean-color measurements from the CZCS are being used in fishery resource applications for (1) the location of ocean fronts, effluents, and circulation features, (2) quantitative determinations of ocean color that are

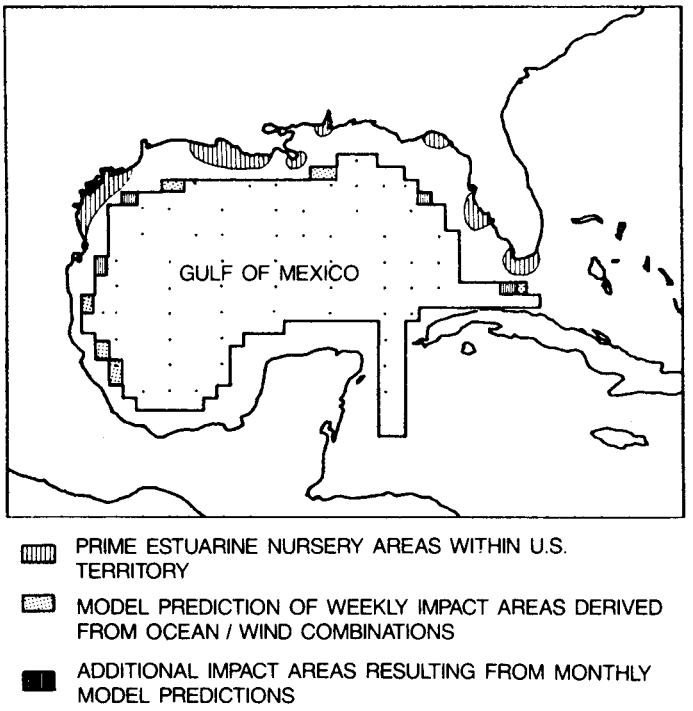

FIG. 10. Predicted coastal recruitment areas compared to known locations of estuarine nursery grounds for shrimp and fishes. (From Brucks *et al.*, 1984.)

directly related to chlorophyll and sestonic concentrations, and (3) the identification of water masses.

2.3.1. Use of CZCS Measurements in Albacore Tuna Studies. Distribution of albacore catches in relation to color boundaries. CZCS imagery and albacore tuna catch data obtained from daily logs submitted by fishermen were used by Laurs *et al.* (1984) to investigate the relationships between albacore fishing success and ocean color boundaries off the U.S. Pacific west coast. The ratios of CZCS channel 1 to channel 3 radiance [blue/green ratio or $R(13)$] were used to determine the locations of ocean color boundaries after atmospheric contamination was removed from the imagery using the algorithm of Smith and Wilson (1981). $R(13)$ was also converted to phytoplankton pigment concentration using the algorithms of Clark (1981) and Smith and Baker (1982). Normalized catch data for 5-day periods, from 2 days before to 2 days after each Nimbus-7 pass, were plotted on the CZCS images.

In nearshore waters color imagery showed a sharp color front marking the boundary between the coastal and oceanic water masses and corresponding to

the temperature front visible in the AVHRR images (see Section 2.1.2). The boundary generally had a meandering north–south distribution with intrusions of oceanic water into coastal water. Chlorophyll concentrations were usually less than 0.30 mg m^{-3} offshore of the color front and were greater than 0.50 mg m^{-3} inshore of the front. Strong color fronts and chlorophyll concentrations > 1.0 mg m^{-3} were also observed in the waters nearer the coast associated with aged upwelled waters. Albacore fishing effort was distributed mostly in the oceanic waters with lesser amounts in the coastal waters. The fishing effort tended to be highest along or in the vicinity of the color boundary separating coastal and oceanic waters and in some cases up to about 100 km from the boundary in oceanic waters. Also, high fishing effort was concentrated in the fingers of oceanic water that intruded into the coastal water. Figure 11 (from Laurs *et al.*, 1984) shows a plot of albacore catch rates superimposed on a false color image of the blue/green color ratio, $R(13)$. The catch rates were highest in the bluish oceanic waters near the color boundary marking the interface between oceanic and coastal waters. The shoreward intrusions of oceanic waters had particularly large catches concentrated at the color boundary. Catch rates within the greenish coastal waters were low or nil. Satellite data and albacore fishery data were also examined from a large oceanic region centered about 500 miles off the coasts of Washington and Oregon. No temperature fronts were visible in AVHRR imagery; however, a diffuse and broken color front was apparent in the center of a CZCS image covering the region. The oceanographic boundary defined by the color front marked an area of high fishing activity and large mean catches in relatively productive water with chlorophyll concentrations of 0.30–0.40 mg m^{-3}. Sea surface temperature was observed to increase gradually from 12 to 20°C over about 8° of latitude.

The satellite images and concurrent albacore catch data examined by Laurs *et al.* (1984) clearly demonstrate that the distribution and availability of albacore are related to oceanic fronts. They also substantiate the conventional wisdom of many fishermen who use temperature and/or color "breaks" to locate potentially productive fishing areas for albacore. The results show that in nearshore regions commercially fishable aggregations of albacore are found in warm, blue oceanic waters near temperature and color fronts on the seaward edge of coastal water masses. Shoreward intrusions of oceanic water are particularly favorable sites for albacore aggregation. In offshore waters during late summer, commercial concentrations of albacore were found associated with oceanic boundaries that are marked by color

FIG. 11. Distribution of mean daily albacore tuna catches made by commercial fishing vessels superimposed on Nimbus-7 CZCS blue/green color ratio and phytoplankton pigment concentration in waters off central California. (From Laurs *et al.*, 1984.)

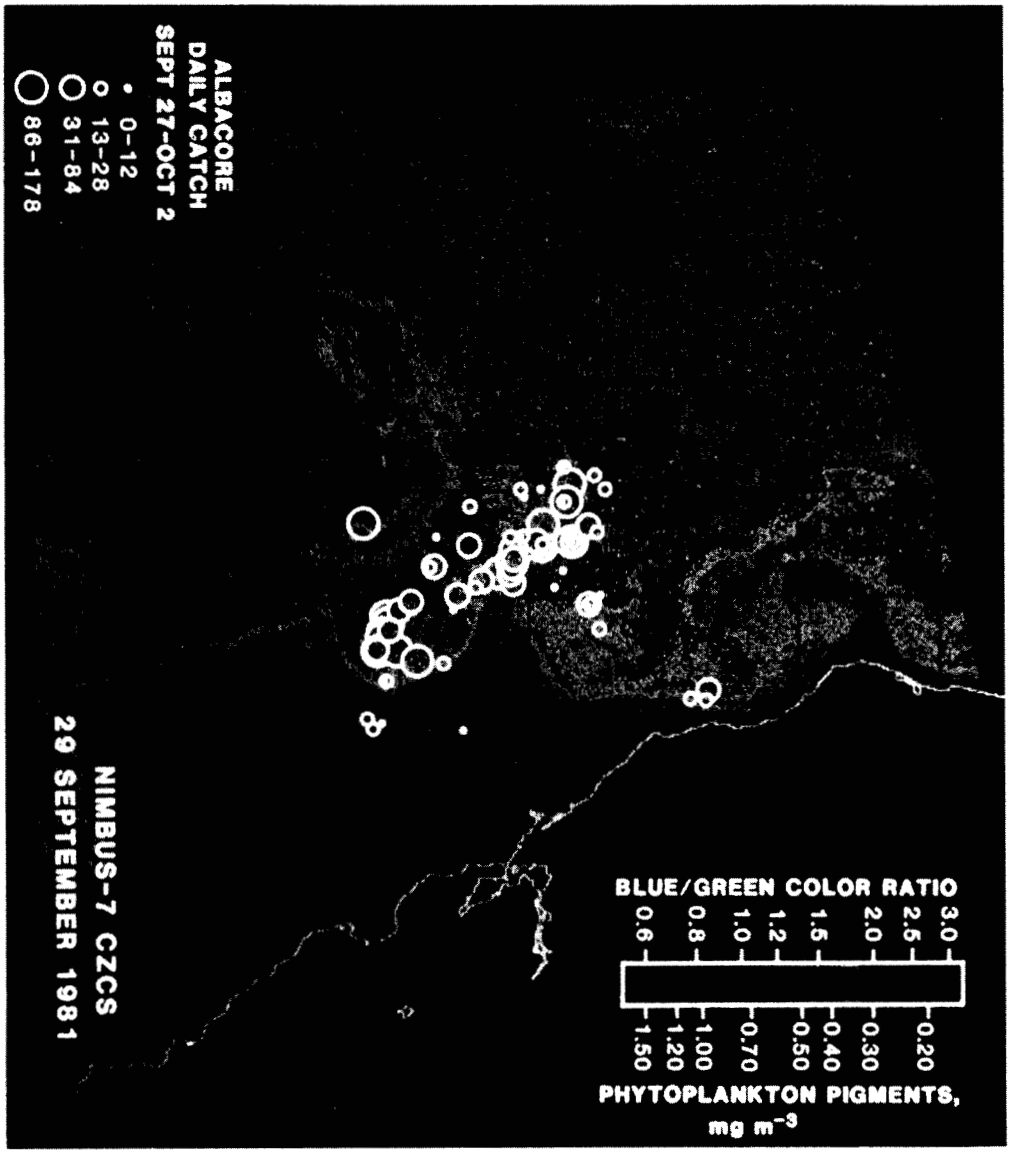
ALBACORE
DAILY CATCH
SEPT 27-OCT 2
0-12
13-28
31-84
86-178
NIMBUS-7 CZCS
29 SEPTEMBER 1981
BLUE/GREEN COLOR RATIO
0.6
0.8
1.0
1.2
1.5
2.0
2.5
3.0
1.50
1.20
1.00
0.70
0.50
0.40
0.30
0.20
PHYTOPLANKTON PIGMENTS,
mg m-3

fronts detectable from satellites but lacking sea surface temperature gradients. The availability of albacore in offshore waters appears to be higher in relatively productive waters. The temperature signature denoting the boundaries of the relatively more productive waters, if present earlier, may be lost due to seasonal warming.

It was noted earlier (Section 2.1.2.1) that Laurs and Austin (1985) speculate that behavior mechanism(s) related to feeding may be responsible for tuna aggregating on the warm side of temperature boundaries. To support this argument, the authors used CZCS measurements along with a knowledge that tuna are visual feeders. The distribution of ocean color boundaries, apparent in CZCS imagery collected concurrently with albacore acoustic tracking, showed a gradient nearly coincident with the sea surface temperature gradient patterns visible in AVHRR imagery. The diffuse attenuation coefficient (k) and chlorophyll concentration measured by the CZCS also showed a similar pattern to the gradient in sea surface temperature, with lower values in the warmer waters and higher values in the cooler waters. All tracked albacore remained in clear, warm oceanic waters and did not cross the boundaries into turbid, cool coastal waters. However, the tracked fish moved vertically through water temperatures that were 3+ times greater than the gradients in surface temperature apparent in the AVHRR imagery (Section 2.1.2.1). These results suggested to the authors that the influence of water clarity on the detection and capture of prey may play a key role in the mechanism(s) underlying the aggregation of tuna on the warm side of ocean fronts. The aggregation of commercial concentration of albacore in clear water on the oceanic side of fronts in nearshore areas found by Laurs *et al.* (1984) may reflect an inability of albacore to capture efficiently large, mobile prey in turbid coastal water and a dependence on food that has migrated or has been dispersed across the coastal–oceanic boundary. In offshore regions, the aggregation of albacore in relatively productive waters presumably occurs because relatively higher amounts of food organisms are present, yet the waters are clear enough for the albacore to detect them.

Studies have shown that both infrared and visible color data from satellites can define environmental limits on the spatial distribution of fishable aggregations of albacore and can do so more effectively than ship or aircraft data as used in the past. No other observational perspective so convincingly reveals the shapes, sizes, and continuity of mesoscale oceanic features, which are important in determining the distribution and availability of this highly migratory species.

2.3.2. Use of CZCS Imagery in a Study of Spawning of the Northern Anchovy. Fiedler (1983) extended the study of Lasker *et al.* (1981) in an investigation of the distribution of northern anchovy spawning observed on

four intensive egg surveys of the Southern California Bight. AVHRR and CZCS data were used to describe mesoscale patterns of sea surface temperature and phytoplankton pigment concentration. Spawning anchovy were excluded from cold (<13.5–14°C) upwelled water to the south of Point Conception, a feature defining the northern boundary of this spawning area. This pattern was observed in February–April 1981 and February 1982, corroborating the results of Lasker *et al.* for April 1980.

Anchovy spawning to the south of San Diego in 1980–1982 was confined to a narrow band along the coast, with occasional extensions farther offshore. Sea surface temperature increased gradually offshore, sometimes exceeding 17°C, but no temperature fronts were observed in the AVHRR imagery to explain the spawning distribution. CZCS images, however, showed relatively high phytoplankton pigment concentrations in a coastal band with a sharp chlorophyll front defining the seaward extent of spawning activity (Fig. 12). In February 1982, spawning extended farther offshore in a jet of cool water with a high pigment concentration.

The spatial distribution of northern anchovy spawning can thus be defined by mesoscale patterns in satellite sea surface temperature and phytoplankton pigment images (Lasker *et al.*, 1981; Fiedler, 1983). While neither parameter alone is sufficient, both together may define the spatial distributions nearly completely. In general, the northern extent of spawning in the Southern California Bight, and the offshore extent north of Santa Catalina Island, are limited by cold, upwelled water advected south of Point Conception (Figs. 1 and 13). Spawning activity to the south is limited by low phytoplankton pigment levels in oceanic water found 20–100 km offshore, rather than by temperature (Fig. 12). However, these factors do not directly determine spawning success. Larval anchovy survival is thought to depend upon aggregations of nutritionally suitable food organisms in a stratified water column (Lasker, 1981). Satellite observations of relatively warm surface temperatures along with moderately high pigment levels may indicate a stratified water column with a mature phytoplankton community dominated by dinoflagellates. On the other hand, a well-mixed water column would be indicated by colder surface temperatures caused by upwelling or storm mixing; unsuitable food conditions would be indicated either by the low phytoplankton pigment levels of unproductive oceanic water or by very high levels associated with surface diatom blooms in recently upwelled water (Fiedler, 1983).

2.3.3. Pelagic Fishery in the Southern Benguela Current. Shannon *et al.* (1983) report on ocean-color experiments conducted off South Africa to relate satellite radiance measurements to the distribution of chlorophyll and to fish shoals. In the study, CZCS images were selected as being representative of seasons and events in the southern Benguela Current. Based on a relatively

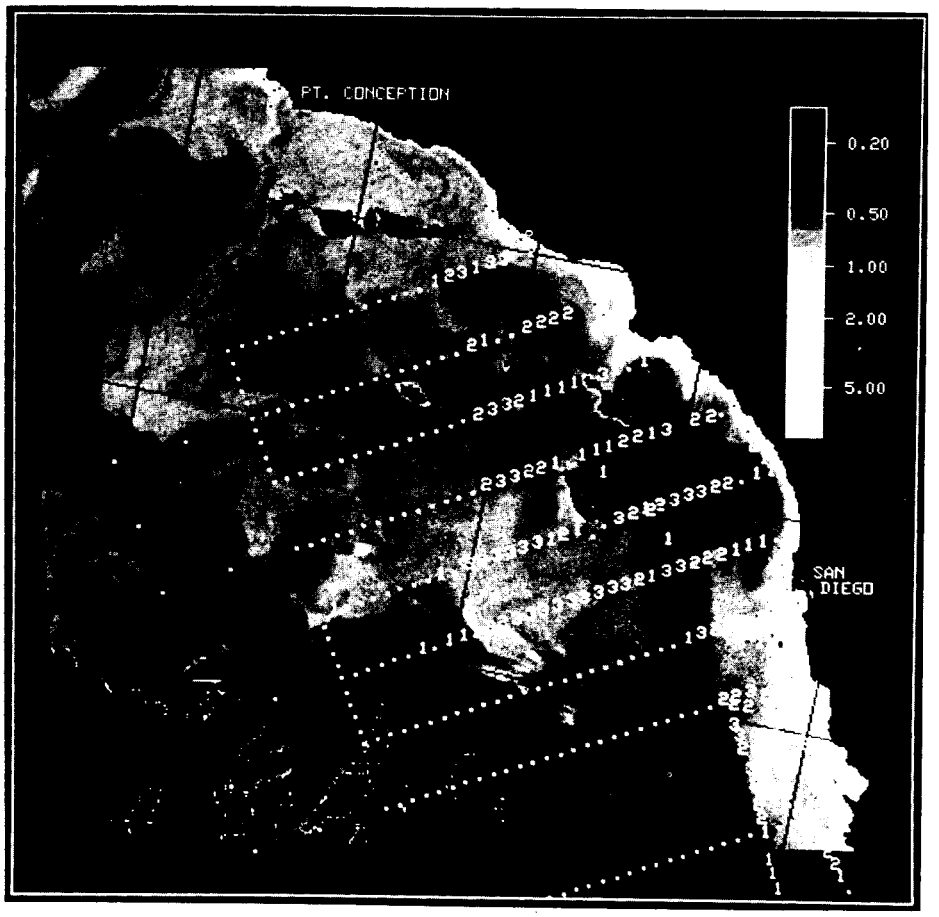

FIG. 12. Distribution of anchovy eggs superimposed on phytoplankton pigments (mg m^{-3}) from Nimbus-7 CZCS for the Southern California Bight. (From Fiedler, 1983.)

high correlation ($r = +0.89$) between near-surface chlorophyll concentrations measured aboard ship and those determined from CZCS data, the authors concluded that the satellite method could be used with confidence in the Benguela Current region to produce contoured fields of chlorophyll concentrations. The chlorophyll distribution patterns deduced from the CZCS radiances were found to be generally consistent with the known distribution and migration patterns of the main pelagic fish species off South Africa. For example, the location of a color front observed in the southern region between Cape Agulhas and Cape Point coincided approximately with the outer limit of the fish-catch locations of the five fish species that comprise the South Africa pelagic fishery.

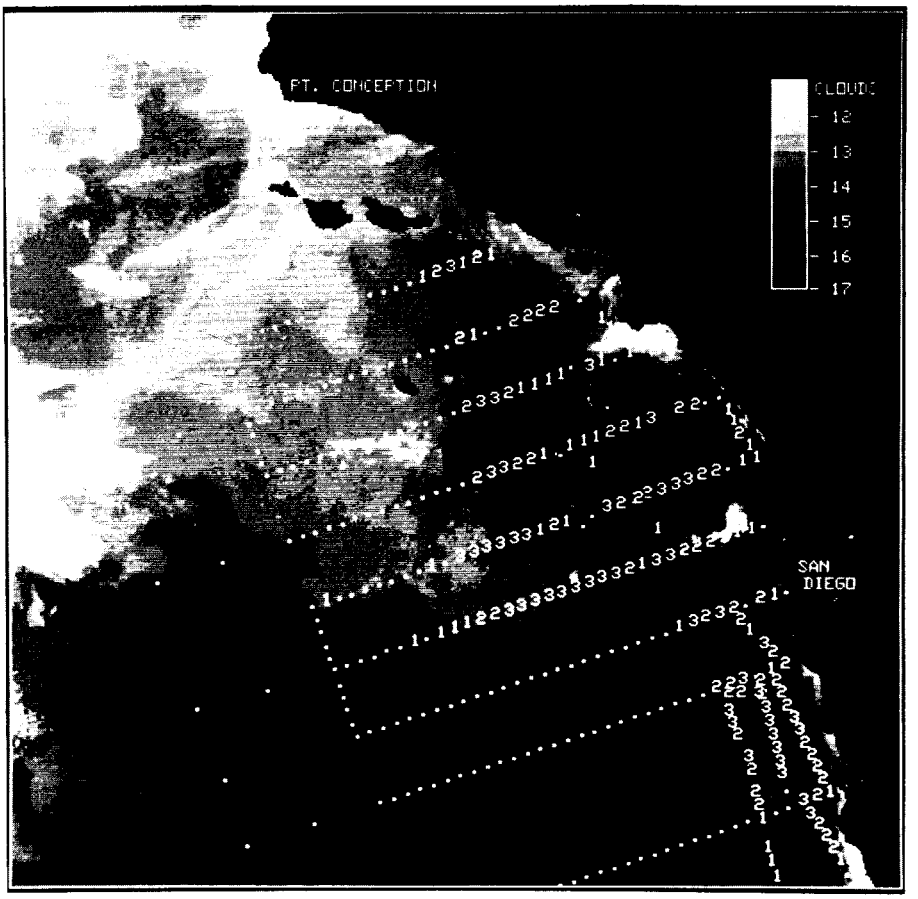

FIG. 13. Distribution of anchovy eggs superimposed on sea surface temperature from NOAA-6 AVHRR for the Southern California Bight. (From Fiedler, 1983.)

The authors caution that before definite conclusions can be drawn about the usefulness of satellite ocean-color imagery for the management of pelagic fish stocks in the southern Benguela Current, more CZCS images must be examined and additional work is needed on the feeding requirements of the different life stages of the various fish species. They do go on to state:

> Nevertheless, it does seem from the information available that the CZCS is a potentially powerful management tool. It could be used to provide an environmental index for fish availability, which in turn could be used to refine CPUE (catch-per-unit-effort) estimates or to direct fishing effort. It is also possible that chlorophyll measured by satellite could be used as a biological environmental input for fish recruitment models. Most certainly the accuracy of chlorophyll determination from satellites is adequate for it to be used in conjunction with thermal imagery and limited *in situ* monitoring to detect anomalous or episodic events [Shannon *et al.*, 1983].

3. Utilization of Satellite Data in Fisheries-Aids Products Distribution to Fishermen

Commercial fishermen have always been concerned about safety at sea and in making the best catch for the amount of time expended in search of productive fishing areas. In the last decade, commercial fishing on the high seas has become an increasingly competitive and economically risky business. To ensure a profit it has become necessary for the fishermen to utilize available technological and scientific knowledge to improve their catches. Accordingly, modern commercial fishermen require timely, reliable, and accurate meteorological and oceanographic information. Although the use of satellite imagery in the preparation of fisheries-aids products has been limited, it has the potential to contribute significantly in meeting the increased needs of fishermen for environmental information.

The first application of satellite-received data in fisheries-aids products was in a program initiated in 1971, wherein San Diego-based purse seine tuna fishermen operating in the eastern tropical Pacific were provided oceanographic and weather products prepared specifically to meet their requirements (Laurs, 1971). The tailored fisheries-aids products were transmitted via radio facsimile to cooperating fishermen on the fishing grounds who in turn radioed ashore surface weather observations and expendable bathythermograph subsurface temperature observations. In this program visual and infrared satellite images received by automatic picture transmission (APT) at the NMFS Laboratory in La Jolla, California, were analyzed in conjunction with surface observations. The APT photos were used to assist in determining the locations and movements of severe weather conditions which affected safety and/or hampered fishing operations. In addition they were used to define the location of the Intertropical Convergence Zone and regions of ocean surface temperature gradients which are important indicators in locating potential fish-productive ocean areas.

Subsequent to this endeavor, other projects and programs have used or are using satellite data in fisheries-aids products which are distributed to fishermen by a variety of mechanisms, including radio facsimile transmission, voice broadcast, U.S. mail, and telephone telecopier. Fiedler *et al.* (1984) review fisheries applications of satellite data in the eastern North Pacific.

3.1. Thermal Boundary Charts

Operational application of satellite data to commercial fishing operations began along the Pacific coast in 1975 (Breaker, 1981). Charts showing the locations of oceanic thermal boundaries are derived from satellite infrared imagery and provided to commercial and recreational fishermen for use in locating potentially productive fishing areas. Initially the charts were

distributed by telephone telecopier and the U.S. mail to locations where fishermen would have the opportunity to examine them before starting a fishing trip. Radiofasimile has also been used to broadcast the charts directly to boats at sea since 1980. The thermal boundary charts are produced by the (1) NOAA Satellite Field Services Station in Redwood City, California, which produces two charts for the area between 28°N and 40°N; (2) NOAA National Ocean Services Center in Seattle, Washington, which produces a chart for the area between 40°N and 52°N; and (3) NOAA Alaska Ocean Services Unit in Anchorage, Alaska, which produces charts covering the area from 48°N to 75°N. Examples of sea surface thermal analysis charts off the Pacific west coast are found in Fig. 14.

The charts are prepared one to three times a week and are distributed primarily by USCG radiofacsimile broadcast. Fishermen use these charts to save time in searching for productive fishing areas associated with frontal features (Short, 1979; Breaker, 1981).

On the east coast, charts depicting oceanographic features and sea surface temperatures derived from satellite infrared thermal imagery and ship reports are available by mail to interested fishermen through the NMFS Atlantic Environmental Group (AEG) in Narragansett, Rhode Island (Chamberlain, 1981). These products are produced from interpretations and detailed environmental analyses done at AEG on the Oceanographic Analysis Charts which are produced routinely as a joint effort by the National Weather Service and National Environmental Satellite, Data, and Information Service (NESDIS). High-resolution infrared images from NOAA GOES satellite and ship reports are used in the preparation of the charts for waters off the Atlantic coast (see Fig. 15). Of particular interest to fishermen, these charts show (1) the offshore limit of shelf-water mass, in which most of the fishery resource species reside, and (2) the numbers, measurements, and persistence of warm-core Gulf Stream rings and the influence of these dynamic deep-ocean features on the relatively shallow waters of the fishing grounds.

NESDIS field stations in Miami, Florida, and Washington, D.C., prepare regionally oriented flow charts of the Gulf Stream from Florida to Maine three times weekly during October through May from GOES infrared images. In addition, a chart is prepared depicting the path of the Loop Current in the Gulf of Mexico from the Mississippi Delta to the east coast of Florida. The charts are distributed in cooperation with Sea Grant marine advisory serivce agents along the Atlantic coast and Gulf of Mexico by mail and telephone telecopiers and in some cases a narrative version is prepared for voice broadcast by local radio stations (Lowry and Leaky, 1982 and Flimlin, 1982). The charts have been particularly useful to lobster fishermen in reducing gear loss due to strong currents of Gulf Stream warm-core eddies, and to swordfish and recreational fishermen (Lowry and Leaky, 1982).

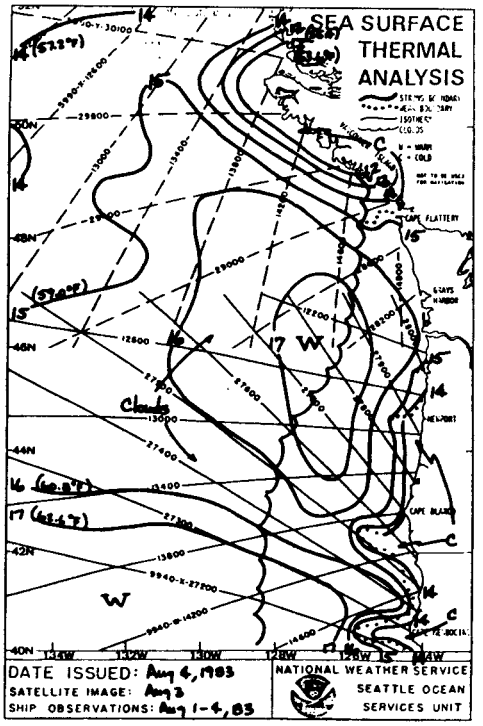

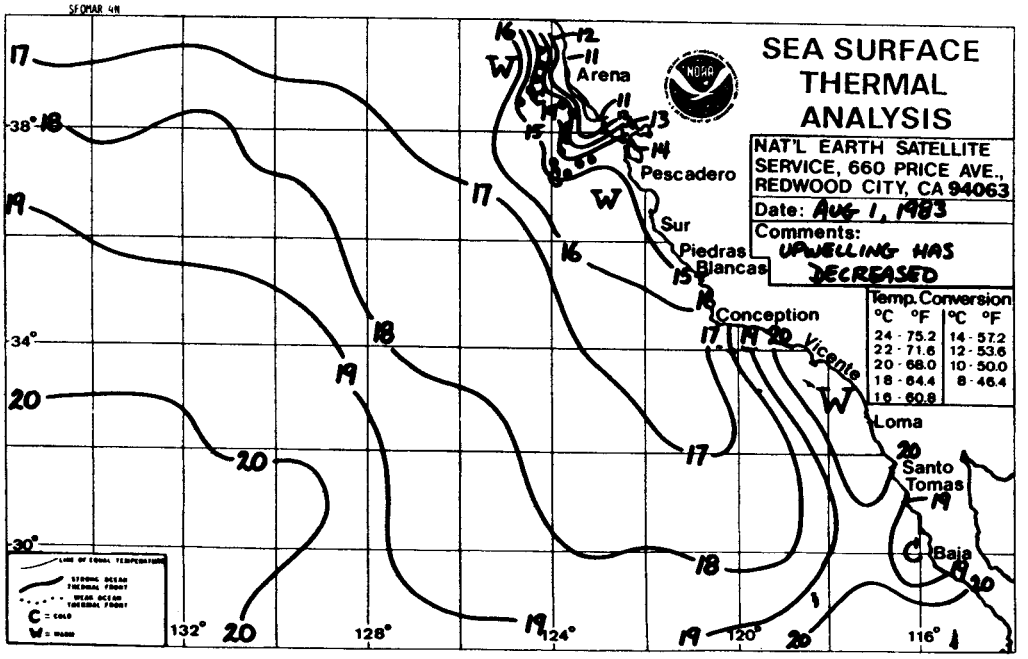

FIG. 14. Ocean frontal analysis charts for waters off the Pacific west coast.

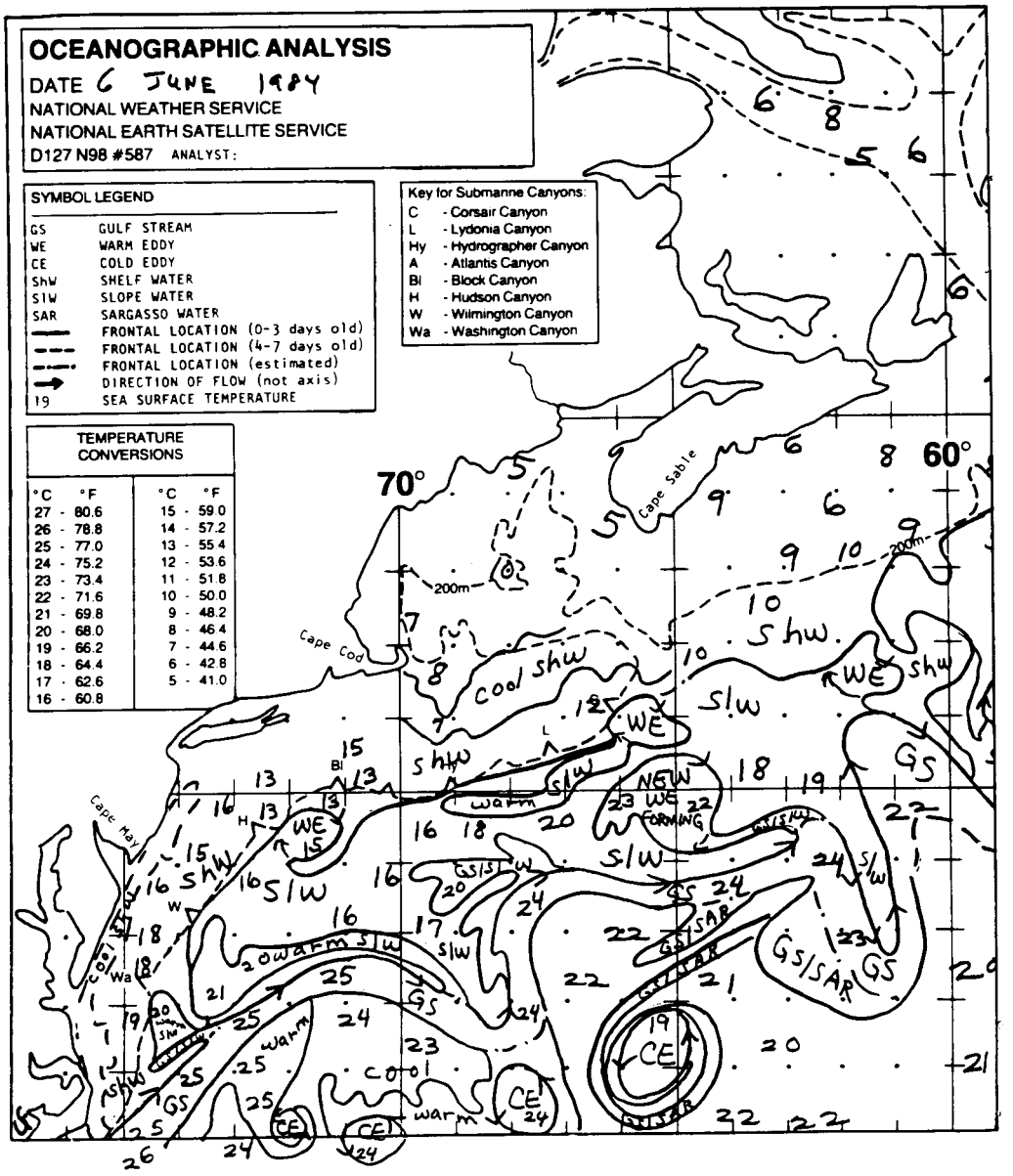

FIG. 15. Ocean frontal analysis chart for waters off the U.S. northeast coast.

3.2. Sea-Ice Forecast Charts

Sea-ice forecast charts derived from Nimbus-7 SMMR and polar-orbiting satellite infrared imagery are prepared by the NOAA Alaska Ocean Services Unit and transmitted by USCG radiofacsimile to fishermen and other marine users. Sea ice is an important seasonal feature in the Alaskan environment that can be monitored by satellite measurements (Weeks, 1981; McNutt, 1981). Sea ice affects commercial fishing activities by threatening vessel safety, limiting navigation and access, and damaging fishing gear. However, sometimes waters near the edge of pack ice can offer shelter or rich fishing grounds.

3.3. NASA/JPL Satellite Data Distribution System and Fisheries Demonstration Program to U.S. West Coast Fisheries

The prime motivation leading to the expanded use of satellite observations in fisheries-aids products has been provided by the Seasat Commercial Demonstration Program (SCDP) sponsored by NASA/JPL.[1] The SCDP offered a unique opportunity to evaluate the use of oceanographic satellite observations for support of commercial fisheries. The program led to the development of an operational Satellite Data Distribution System (SDDS) used to distribute oceanographic products to various components of the oceanographic user community (Montgomery, 1981). The distribution of products to fishermen included transmission of fishery advisory charts via radiofacsimile to tuna purse seiners operating in the eastern tropical Pacific, albacore tuna and salmon fishing vessels working along the Pacific west coast, and king crab vessels fishing in the Bering Sea.

The SDDS was planned and initially designed to distribute to marine users oceanographic products derived from measurements made by Seasat. When the Seasat prematurely failed, an alternative plan was devised to distribute subsets of the basic marine numerical analyses prepared at Navy Fleet Numerical Oceanographic Center (FNOC) in Monterey, California. The SDDS serves as a pilot demonstration from which general system requirements are being developed for future operational ocean-oriented satellite programs. The system also provides support for limited real-time experiments that test the utility of satellite observations in various maritime applications, including fisheries. The SDDS became operational in 1979 with products

[1] Capt. Paul M. Wolff (USN Retired) has played a key role in the development of operational techniques to integrate satellite observations of the ocean with conventional data to produce unique environmental charts for use by commercial fishermen.

originating at FNOC. For fisheries users, the products consisted of numerically analyzed fields of winds, waves, and sea surface temperature. Although these products were operationally useful, they contained few or no satellite measurements and they were not tailored toward specific fisheries applications. Nevertheless, fishermen who utilized the products and kept evaluation logs estimated a 10–15% savings in search time as the result of using the products (Hubert, 1981).

In 1981, a plan was adopted to distribute new fisheries support products which built upon the existing SDDS system. The new products were tailored toward specific fisheries applications. They were prepared using a man/computer mix wherein additional knowledge and information, including satellite measurement, were incorporated. The program involved cooperative facilities and expertise in government, university, and commercial organizations. A schematic drawing showing the data sources and routing of the experimental fisheries-aids products, taken from Montgomery (1981), is given in Fig. 16.

Beginning in 1983, the responsibility for preparation of most of the marine advisory products was transferred to the NOAA National Ocean Service. Charts continue to be distributed to fishermen at sea by the radiofacsimile facilities shown in Fig. 15. However, except for the thermal boundary charts (Section 3.1), the products are now in a format for general use by marine users.

3.3.1. Ocean Color-Boundary Charts. Experimental ocean-color boundary charts based on Nimbus-7 CZCS imagery are distributed to U.S. West Coast fishermen under the auspices of the NASA/JPL Fisheries Demonstration Program (Montgomery, 1981). These charts (see example in Fig. 17) delineate strong gradients in the blue/green color ratio (channel 1/channel 3 radiances). They are produced at almost weekly intervals depending on cloud conditions, and cover coastal areas up to 700,000 km^2 between Guadalupe Island and Vancouver Island. Nimbus-7 CZCS passes along the Pacific coast are collected at the Scripps Institution of Oceanography (SIO) Satellite Oceanography Facility, processed in near-real time at the SIO Visibility Laboratory and transmitted by radiofacsimile the following day to fishing boats at sea from radio station WWD in La Jolla, California. Color photographs of the satellite images are also distributed by express mail to various fishing ports and to Sea Grant marine advisors in daily contact with fishermen. The color boundary charts and photographs are used primarily by commercial albacore and salmon fishermen, and recreational fishermen in southern California. Fishermen use the color boundary charts to locate color gradients or "breaks" which are important in determining potentially productive fishing areas.

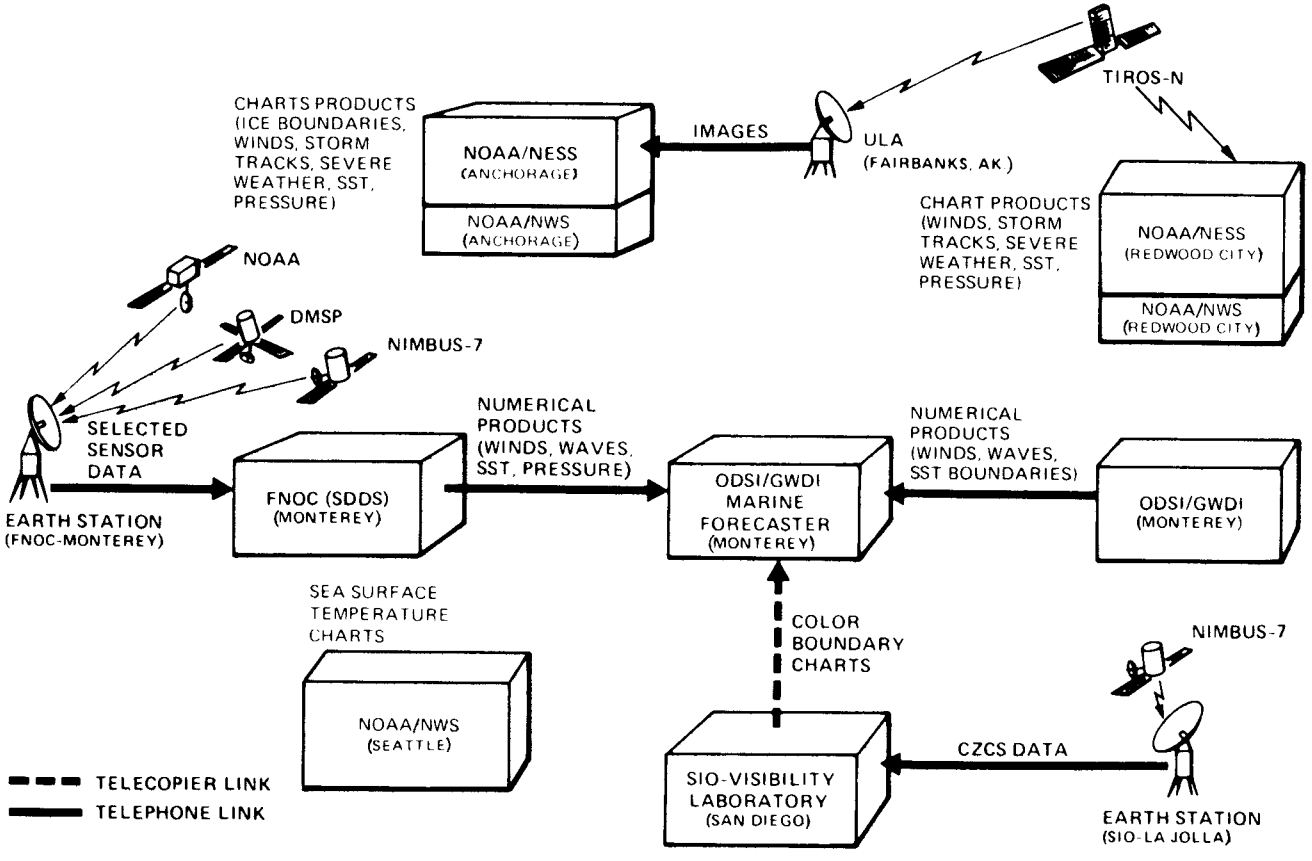

FIG. 16. Data sources and monitoring of experimental fisheries-aids products for the NASA/JPL Fisheries Demonstration Program to the U.S. West Coast fisheries. (From Montgomery, 1981.)

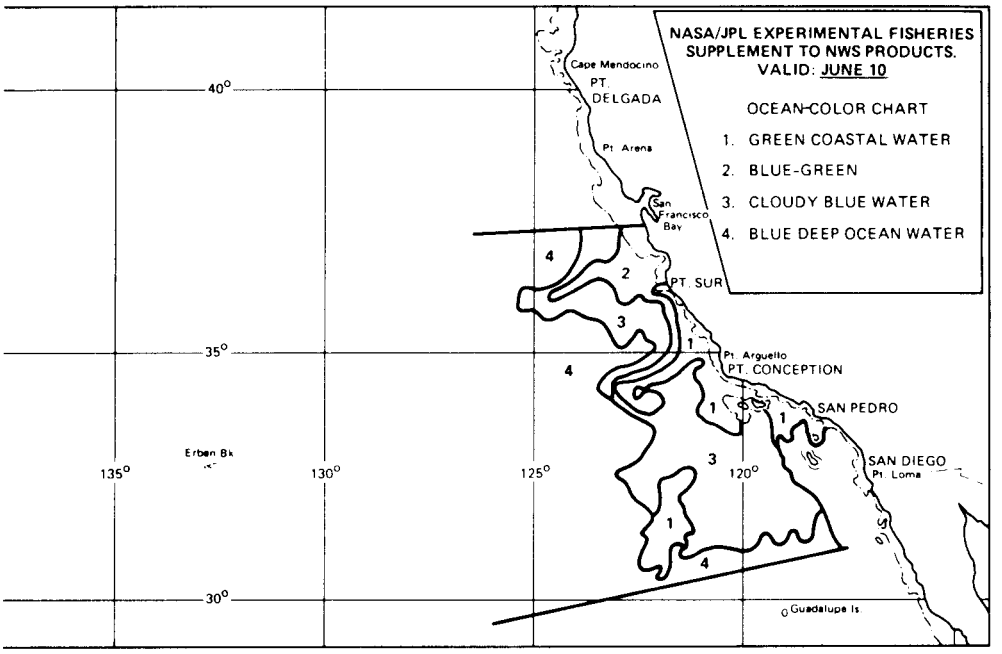

FIG. 17. Nimbus-7 CZCS-derived ocean-color chart tailored for commercial fishing applications. (From Montgomery, 1981.)

REFERENCES

Breaker, L. C. (1981). The application of satellite remote sensing to west coast fisheries. *J. Mar. Tech. Soc.* **15,** 32–40.

Brucks, J. T., Butler, J. A., Faller, K. H., Holley, H. J., Kemmerer, A. J., Leming, T. D., Savastano, K. J., and Vanselous, T. M. (1977). LANDSAT menhaden and thread herring resources investigation, final report. *NOAA, Nat. Mar. Fish. Serv., Southeast Fish. Center* Contr. No. 77-16F.

Brucks, J. T., Leming, T. D., and Burkett, S. B., Jr. (1984). A model investigation using high resolution SASS wind stress measurements to derive wind driven surface layer transport properties in the Gulf of Mexico. *NOAA Tech. Rep.* In press.

Carey, F. G., and Robinson, B. H. (1981). Daily patterns in the activities of swordfish, *Ziphias gladuis,* observed by acoustic telemetry. *Fish. Bull., U.S.* **79,** 277–292.

Chamberlain, J. L. (1981). Application of satellite infrared data to analysis of ocen frontal movements and water mass interactions off the northeast coast. *NW Atlantic Fish. Organ. NAFO Scr. Doc. 81/IX/123, Ser. No. 429.*

Clark, D. K. (1981). Phytoplankton pigment algorithms for the NIMBUS-7 CZCS. *In* "Oceanography from Space" (J. F. R. Gower, ed.), pp. 227–238. Plenum Press, New York.

Cram, D. L. (1979). A role for the NIMBUS-6 Coastal Zone Color Scanner in the management of a pelagic fishery. *Fish. Bull. S. Afr.* **11,** 1–9.

Ekman, V. W. (1905). On the Influence of the earth's rotation on ocean currents. *Ark. Mat. Astron. Fys.* 2, 1–53.

Fiedler, P. C. (1983). Satellite remote sensing of the habitat of spawning anchovy in the Southern California Bight. *CalCOFI Rep.* **24,** 202–209.

Fiedler, P. C. (1984a). Some effects of El Niño 1983 on the northern anchovy. *CalCOFI Rep.* **25,** 53–58.

Fiedler, P. C. (1984b). Satellite observations of El Niño along the U.S. Pacific coast. *Science* **224,** 1251–1254.

Fiedler, P. C., Smith, G. B., and Laurs, R. M. (1984). Fisheries applications of satellite data in the eastern North Pacific. *Mar. Fish. Rev.* **46**(3), 1–13.

Flimlin, G. (1982). A call saves time and fuel. *Sea Grant Today* **12,** 6.

Hela, L., and Laevastu, T. (1961). Fisheries hydrography. *Fish. News (London).*

Hela, L., and Laevastu, T. (1970). Fisheries oceanography. *Fish. News (London).*

Hubert, W. (1981). An evaluation of the utility of Seasat data to ocean industries. Final Report, Seasat Commercial Demonstration Program. *Jet Propulsion Laboratory Document No. 622-225.*

Kemmerer, A. J., Benigno, J. A., Reese, G. B., and Minkler, F. C. (1974). Summary of selected early results from ERTS-1 Menhadden experiment. *Fish. Bull.* **72,** 375–389.

Lasker, R. (1978). The relation between oceanographic conditions and larval anchovy food in the California Current: Identification of factors contributing to recruitment failure. *Rapp. P. v. Re'un. Cons. Int. Explor. Mer.* **173,** 212–230.

Lasker, R. (1981). Factors contributing to variable recruitment of the northern anchovy (*Engraulis mordax*) in the California Current: Contrasting years, 1975–1978. *Rapp. P. v. Re'un Cons. Int. Mer.* **179,** 375–388.

Lasker, R., Peláez, J., and Laurs, R. M. (1981). The use of satellite infrared imagery for describing ocean processes in relation to spawning of the northern anchovy (*Engraulis mordax*). *Remote Sens. Environ.* **11,** 439–453.

Laurs, R. M. (1971). Fishery-advisory information available to tropical Pacific tuna fleet via radio facsimile broadcast. *Comm. Fish. Rev.* **33,** 40–42.

Laurs, R. M., and Austin, R. (1984). Small-scale movements of albacore tuna in relation to oceanic frontal features observed in satellite. In preparation.

Laurs, R. M., Yuen, H. S. H., and Johnson, J. H. (1977). Small-scale movements of albacore, *Thunnus alalunga,* in relation to ocean features as indicated by ultrasonic tracking and oceanographic sampling. *Fish. Bull. U.S.* **73,** 347–355.

Laurs, R. M., Lynn, R. J., Nishimoto, R., and Dotson, R. (1981). Albacore trolling and longline exploration in eastern North Pacific waters during mid-winter 1981. *NOAA Tech. Memo. NMFS, NOAA-TM-NMFS-SWFC-10.*

Laurs, R. M., Fiedler, P. C., and Montgomery, D. C. (1984). Albacore tuna catch distributions relative to environmental features observed from satellite. *Deep-Sea Res.* **31**(6).

Leming, T. D. (1981). Ocean pelagics remote sensing applications. *Interim. Rep. NMFS* Intern. Document.

Lowry, B., and Leaky, T. (1982). Cooperation produces a flow of Gulf Stream information. *Sea Grant Today* **12,** 3–5.

McNutt, S. L. (1981). Remote sensing analysis of ice growth and distribution in the eastern Bering Sea. *In* "The Eastern Bering Sea Shelf: Oceanography and Resources (D. W. Hood and J. A. Calder, eds.), Vol. pp. 1, 141–165. U.S. Govt. Printing Office, Washington, D. C.

Maul, G. A., Williams, F., Roeffer, M., and Sousa, F. (1984). Remotely sensed patterns and variability of bluefin tuna catch in the Gulf of Mexico. *Oceanol. Acta* 7(4), 469–480.

Montgomery, D. R. (1981). Commercial applications of satellite oceanography. *Oceanus* **24,** 56–65.

Neill, W. H. (1976). Mechanisms of behavioral thermoregulation in fishes. Report of Workshop on the Impact of Thermal Power Plant Cooling Systems in Aquatic Environments. *Electric Power Res. Inst. Spec. Rep.* **38,** 156–169.

Parrish, R. H., and MacCall, A. D. (1978). Climatic variation and exploitation in the Pacific mackerel fishery. *Calif. Dept. Fish. Game, Fish. Bull.* **167,** 1–110.

Pearcy, W. G. (1973). Albacore oceanography off Oregon—1970. *Fish. Bull.* **71,** 489–504.

Roffer, M., Carl, M., and Williams, F. (1982). Atlantic bluefin tuna-oceanography-remote sensing. *Proc. Annu. Tuna Conf., 32nd, Inter-Am. Trop. Tuna Comm., La Jolla,* Ca.

Savastano, K. J., Pastula, E. J., Jr., Woods, E. G., and Faller, K. J. (1974). Preliminary results of fisheries investigation associated with Skylab-3. *Int. Symp. Remote Sens. Environ., 9th, Environ. Res. Inst. Mich.* (unpublished report).

Sette, O. E. (1961). Problems in fish population fluctuations. *CalCOFI Rep.* **8,** 21–24.

Shannon, L. V., Mostert, S. A., Walters, N. M., and Anderson, F. P. (1983). Chlorophyll concentrations in the southern Benguela current regions as determined by satellite (NIMBUS-7 Coastal zone colour scanner). *J. Plankton Res.* **5,** 565–583.

Short, K. (1979). How satellites can help you catch more fish and cut costs. *Natl. Fisherman* **60,** 38–39.

Smith, R. C., and Baker, K. S. (1982). Oceanic chlorophyll concentration as determined by satellite (NIMBUS-7 Coastal Zone Color Scanner). *Mar. Biol.* **66,** 269–279.

Smith, R. C., and Wilson, W. H. (1981). Ship and satellite bio-optical research in the California Bight. *In* "Oceanography from Space" (J. F. R. Gower, ed.), pp. 281–294. Plenum, New York.

Squire, J. L., Jr. (1961). Aerial fish spotting in the United States commercial fisheries. *Comm. Tech. Rev.* **23,** 1–7.

Squire, J. L., Jr. (1972). Apparent abundances of some pelagic marine fishes off the southern and central California coast as surveyed by an airborne monitoring program. *Tech. Bull. U.S.* **70,** 1005–1019.

Squire, J. L., Jr. (1982). Catch temperature for some important marine species off California: *NOAA Tech. Rep.* NMFS SSRF-759.

Thomas, J. P. (1981). Assessment of superflux relative to fisheries research and monitoring. *In* "Chesapeake Bay Plume Study" (J. W. Campbell and J. P. Thomas, eds.), *NASA Conf. Publ.* **2188,** 503–509.

Weeks, W. F. (1981). Sea ice: The potential of remote sensing. *Oceanus* **24,** 39–48.